Institute of Medicine and Drug Research, Qiqihar Medical University, Qiqihar, China

Hyaluronic acid-coated single-walled carbon nanotubes loaded with doxorubicin for the treatment of breast cancer

Dan Liu[#], Qi Zhang[#], Jing Wang, Li Fan, Wenquan Zhu, Defu Cai*

Received August 23, 2018, accepted December 14, 2018

**Corresponding author: Defu Cai, Institute of Medicine and Drug Research, Qiqihar Medical University, NO.333, Bukui Street, Jianhua District, Qiqihar, Heilongjiang Province, 161006, P.R. China*
cai@qmu.edu.cn
[#]Co-first authors

Pharmazie 74: 83–90 (2019) *doi: 10.1691/ph.2019.8152*

Hyaluronic acid (HA)-modified amino single-walled carbon nanotubes (NH_2-SWCNTs) were developed for targeted delivery of doxorubicin (DOX) to improve breast cancer treatment. HA, which specifically binds to the CD44 receptor, was non-covalently coated on NH_2-SWCNTs through simply electrostatic adsorption. The formed SWCNTs-DOX-HA complexes were characterized in terms of morphology, particle size and zeta potential by different techniques. The DOX loading percentage on the SWCNTs-DOX-HA complexes was 81.5±1.0 %. *In vitro* release study showed that the release of DOX was pH-triggered and was faster at a lower pH 5.5 (tumor cell micro-environment) than that under physiological conditions (pH 7.4), which was beneficial for intracellular drug release. The SWCNTs-DOX-HA showed a significantly improved intracellular delivery of DOX in CD44 overexpressing MDA-MB-231 cells by flow cytometry and confocal microscopy. Of particular importance, the SWCNTs-DOX-HA complexes were better than the unmodified SWCNTs-DOX on inhibiting proliferation and inducing apoptosis of cells. In addition, the migration of MDA-MB-231 cells was significantly blocked by SWCNTs-DOX-HA. In the cancer cell spheroids assay, SWCNTs-DOX-HA exhibited notable effect to inhibit the growth of cancer cell spheroids. All these results indicated that this developed SWCNTs-DOX-HA complexes hold a great promise to be used as an efficient nano-sized anticancer drug formulation for tumor-targeted treatment.

1. Introduction

Breast cancer is one of the most common and the main reason of deaths among women all over the world. Based on the statistics of American Cancer Society, about 246,660 new cases of breast cancer were diagnosed and 40,450 cases of invasive breast cancer were died in females in 2016 (Singh et al. 2017). Chemotherapy, which uses chemical drugs as anticancer agents to kill cancer cells, is a conventional and effective strategy for fighting against breast cancer in clinical treatment (Assanhou et al. 2015; Zhou et al. 2013). Doxorubicin (DOX), a typical anthracycline antibiotic, is one of the most efficient chemotherapy drugs for the treatment of breast cancer. However, due to lack of tumor targeting, DOX always kill normal cells as well as breast cancer cells, resulting in serious side effects and even potentially life-threatening. The very high toxicity levels often involved in the use of DOX prompted the generation of targeted drug carrier able to release the drug into cancerous cells or tumor tissues, minimizing its distribution and toxicity in healthy tissues (Pistone et al. 2016).

The rapid development of nanomedicine and nanobiotechnology has generated various nano-sized drug carriers in the past few years. Due to the "enhanced permeability and retention" (EPR) effect, nano-carrier could extravasate (escape) into the tumor tissues via the leaky vessels. Thus, the chemotherapy drugs loaded into these nano-sized drug carriers could be accumulated and retained in tumor sites (Schroeder et al. 2012; She et al. 2013). Many drug delivery systems, such as polymeric nanoparticles, dendrimers, liposomes and micelles have been employed to achieve the specific targeting drug delivery, decrease the toxicity and enhance the antitumor efficacy of DOX (Cai et al. 2014; Wen et al. 2018; Xu et al. 2013).

Among the different classes of nano-carriers, single-walled carbon nanotubes (SWCNTs) have excellent biocompatibility, a hollow construction, ultrahigh surface area, tuneable surface chemistry, and stable physical and chemical properties (Dvash et al. 2013; Mehra et al. 2014; Mo et al. 2015; Zhang et al. 2017; Zhang et al. 2009; Zhou et al. 2012). These provide excellent opportunities for use of SWCNTs in both drug delivery and antitumor therapeutics. SWCNTs have the bilayer graphene construction, which make SWCNTs to combine with DOX by π–π stacking interactions, van der Waals interactions, and hydrophobic interactions (Ji et al. 2012; Mehra et al. 2014; Yu et al. 2016; Zhou et al. 2012). SWCNTs can also avoid the drug enzymatic degradation before it enters cancer cells by loading drug inside the tube (Mousavi et al. 2013). However, despite their excellent properties, the wide application of SWCNTs have been hindered by highly hydrophobic, non-targeted cytotoxicity, limited control, and the potential to cause inflammatory and fibrotic reactions (Cao et al. 2015; Chen et al. 2012; Firme and Bandaru 2010; Ji et al. 2012; Liu et al. 2008; Zhang et al. 2009).

In many cases, to resolve the poor aqueous dispersibility and high aggregation tendency of pristine SWCNTs, appropriate surface functionalization by either noncovalent or covalent modification are necessary, which render the SWCNTs water soluble and highly biocompatible (Cao et al. 2015). Modified the SWCNTs with amino groups is a good way enhancing hydrophilicity and reducing the toxicity of SWCNTs (Stevens 2003). More important, further functionalized the SWCNTs with targeting ligands can improve targeting cell recognition and enhance cellular uptake for the drugs, and thus promote antitumor therapeutic efficacy.

Hyaluronic acid (HA), a linear polysaccharide, consists of repeating D-glucuronic acid and N-acetyl-D-glucosamine disaccharide units. HA possesses unique and favorable physicochemical properties, such as biocompatibility, biodegradability, low cytotoxicity and non-immunotoxicity. Additionally, HA is endowed with tumor-specific targeting properties due to its high affinity toward CD44, a cell adhesion membrane glycoprotein overexpressed

on the surface of many cancer cells. Thus, HA can specifically recognize CD44 and has been identified as an effective targeting ligand of tumors which possessed CD44 overexpressing cells (Lin Hou and Zhang 2017; Ouasti et al. 2012). HA has been widely used as a targeting ligand in nanoparticles, micelles, liposomes and polymersomes for cancer targeting drug delivery systems (Huang et al. 2014; Li et al. 2014; Qhattal and Liu 2011; Yanhua Liu 2011). In addition, HA is hydrophilic, which can prolong drug delivery system circulation in the blood and increase accumulation of drug in tumor tissue (Peer and Margalit 2004).

Hence, in the present study, we developed a targeting drug delivery system (SWCNTs-DOX-HA) using amino single-walled carbon nanotubes (NH_2-SWCNTs) as drug carriers, DOX as anti-cancer agent and HA as targeting ligand for treatment of breast cancer. At first, the size of NH_2-SWCNTs was reduced by Nano DeBEE ultra high pressure homogenizer, then, DOX was loaded on NH_2-SWCNTs by utilization of π–π stacking interactions. At last, the SWCNTs-DOX complexes were further non-covalently wrapped with HA through electrostatic adsorption to improve aqueous solubility, prolong blood circulation and realize selective target delivery. The formed SWCNTs-DOX-HA complexes were characterized using different methods. The DOX release behaviors from SWCNTs-DOX-HA were investigated under different pH conditions corresponding to the physiological environments. The targeting efficacy of the SWCNTs-DOX-HA to tumor cells was investigated by intracellular uptake through flow cytometry and confocal microscopy analysis in the MDA-MB-231 cells. The *in vitro* antitumor activities of SWCNTs-DOX-HA were then confirmed in cytotoxicity, apoptosis and migration studies. In addition, a cancer cell spheroid assay was carried out to further estimate the antitumor efficacy of SWCNTs-DOX-HA.

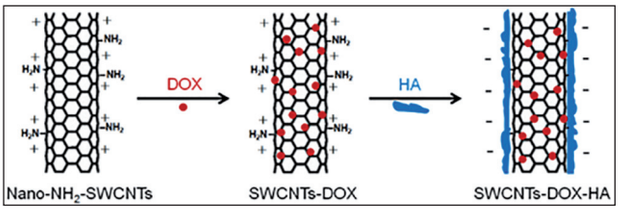

Scheme: Schematic of the preparation process of SWCNTs-DOX-HA.

Table: Characterization of functionalized SWCNTs (mean±SD, *n* = 3)

Samples	Size (nm)	PDI	Zeta potential (mV)	EE (%)
Pristine NH_2-SWCNTs	69187.8±1.9	1.053±0.065	5.05±0.08	
Nano-NH_2-SWCNTs	1838.8±2.3	0.964±0.036	5.86±0.22	
SWCNTs-DOX	2040.4±1.6	0.449±0.017	24.06±0.45	
SWCNTs-DOX-HA	362.5±0.9	0.174±0.043	-55.73±0.89	81.5±1.0

markedly. A lot of dark dots appeared on the surface of tubes and some inside the tubes, which indicated that DOX was loaded on the Nano-NH_2-SWCNTs. Following modification with HA, the surface of SWCNTs was rough and the diameter was larger. The SWCNTs-DOX-HA showed an obvious contrast between the polysaccharide layers and the hollow tubes, indicating the core-shell structures of SWCNTs-DOX-HA (Fig. 1D).

The particle size, zeta potential of series SWCNTs are shown in Table. The surface potentials of the NH_2-SWCNTs and Nano-NH_2-SWCNTs were 5.05±0.08 and 5.86±0.22 mV as the presence of surface amino groups. After loading DOX onto the Nano-NH_2-SWCNTs, the potential increased to 24.06±0.45 mV. After further modification with the negatively charged HA onto the SWNTs-DOX, the zeta potentials dramatic decreased to -55.73±0.89 mV. The particle size of pristine NH_2-SWCNTs was 69187.8±1.9 nm. After dealing with Nano De BEE ultra high pressure homogenizer, the size reduced sharply to 1838.8±2.3 nm. It demonstrated that the application of a nano homogenizer was an effective way to reduce

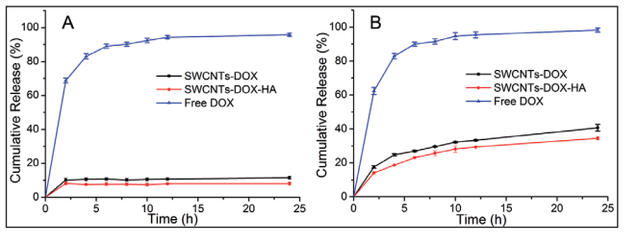

Fig. 2: Release profiles of DOX from free DOX, SWCNTs-DOX and SWCNTs-DOX-HA complexes under different pH conditions. (A) pH 7.4 PBS and (B) pH 5.5 PBS. Each bar denotes mean ±SD, (*n*=3).

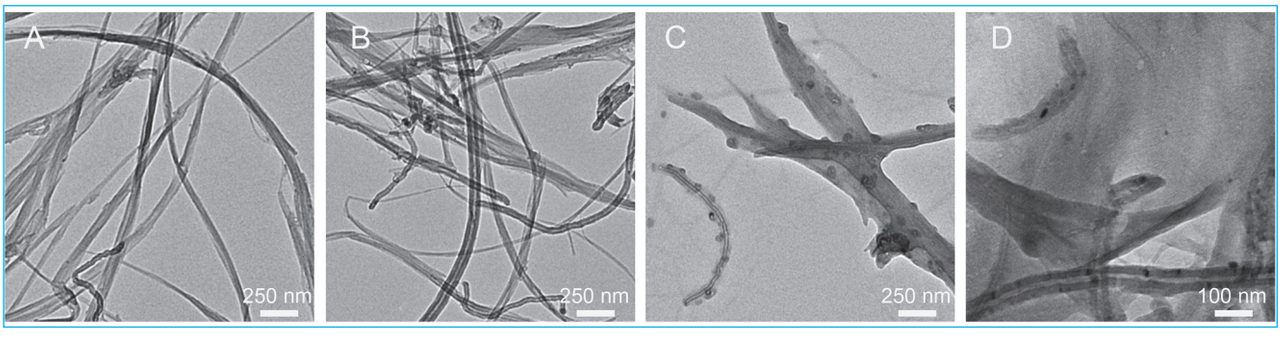

Fig. 1: TEM images of functionalized SWCNTs. (A) Pristine NH_2-SWCNTs; (B) Nano-NH_2-SWCNTs; (C) SWCNTs-DOX; (D) SWCNTs-DOX-HA.

2. Investigations and results

2.1. Preparation and characterization of SWCNTs drug delivery systems

A schematic representation of SWCNTs-DOX-HA complexes is shown in the Scheme. The morphologies of the samples occurred after the several functionalization steps were observed by TEM. Pristine NH_2-SWCNTs (Fig. 1A) exhibited long entangled tubes with smooth surfaces. After treatment by Nano DeBEE ultra high pressure homogenizer, the obtained Nano-NH_2-SWCNTs (Fig. 1B) were generally short. When DOX was loaded on Nano-NH_2-SWCNTs, the morphology of SWCNTs-DOX (Fig. 1C) changed the particles size of SWCNTs. The sizes of Nano-NH_2-SWCNTs and SWCNTs-DOX were around 2000 nm, which were much larger than those observed by TEM. Interestingly, after coated with HA, the size of SWCNTs-DOX-HA obviously reduced to 362.5±0.9 nm. The polydispersity index (PDI) value of SWCNTs-DOX-HA was 0.174±0.043. The DOX loading percentage was 81.5±1.0 %.

2.2. DOX release from the SWCNTs drug delivery systems

The *in vitro* release curves of DOX are shown in Fig. 2. Unlike the fast release of free DOX, the release of DOX from SWCNTs was delayed and pH-triggered. In pH 7.4 PBS (Fig. 2A), the release rates of DOX

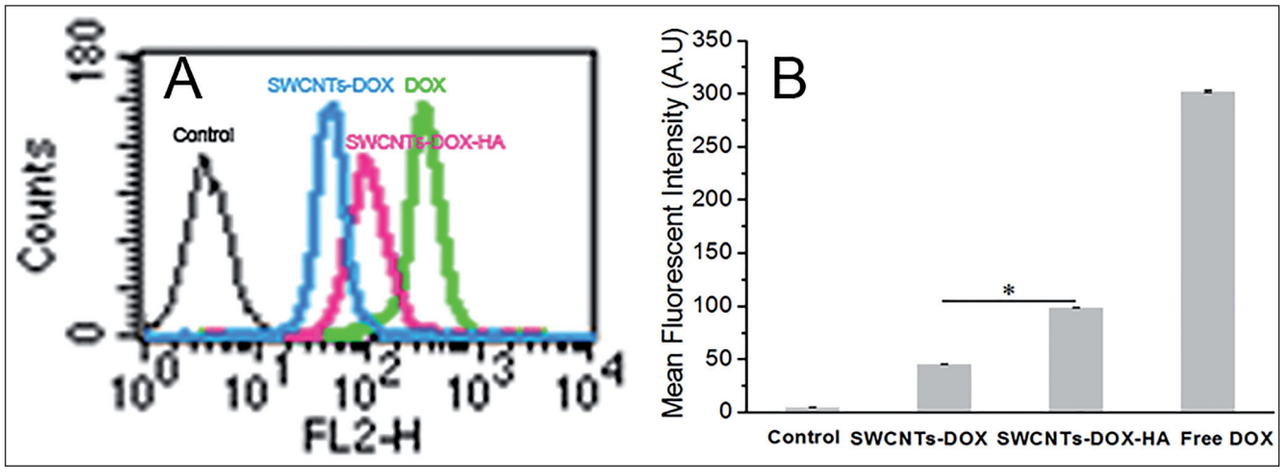

Fig. 3: (A) Flow cytometric data of DOX uptake by MDA-MB-231 cells; (B) Mean fluorescence intensity of MDA-MB-231 cells. Each bar denotes mean ±SD, (n=3). *p<0.01.

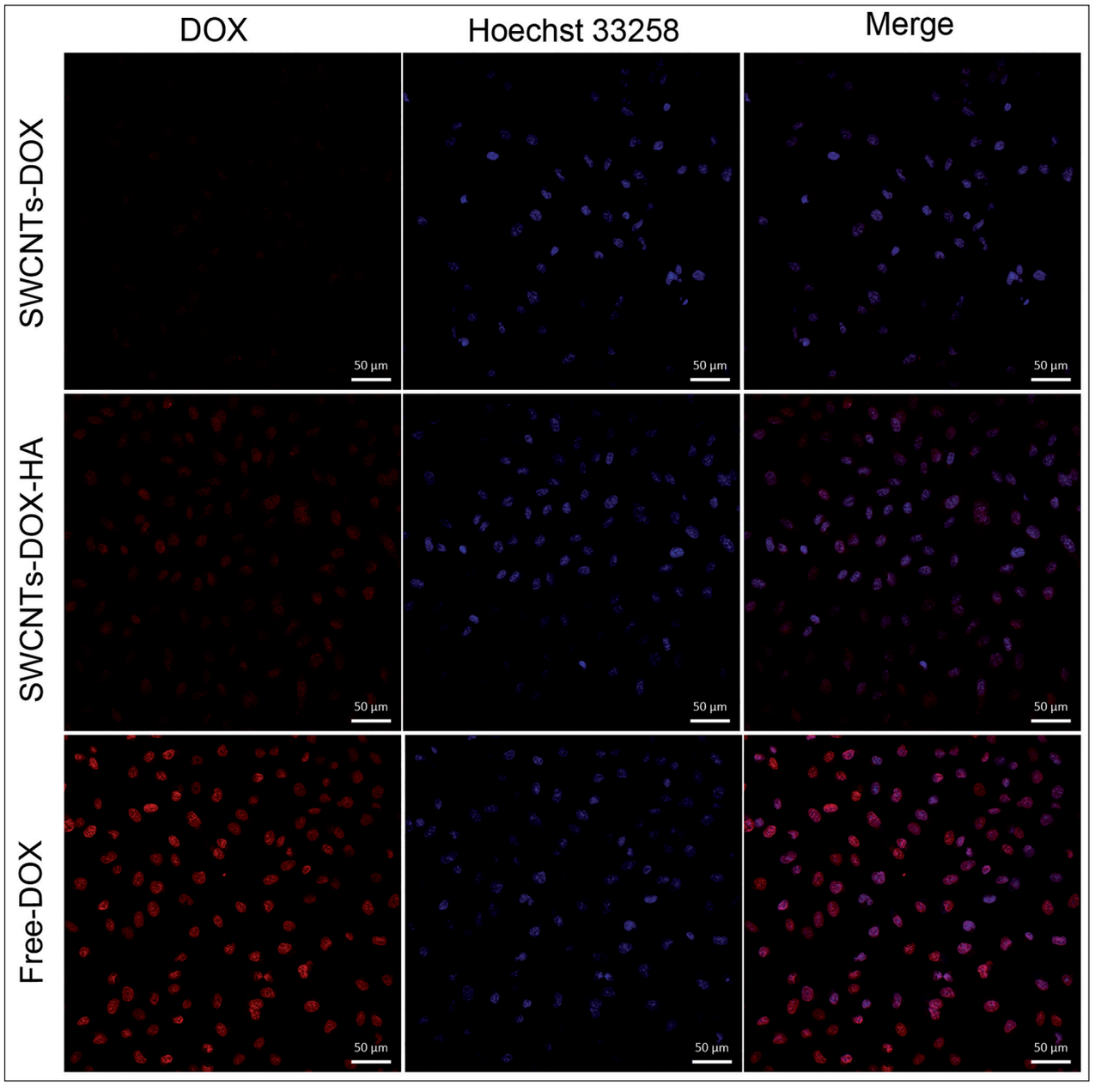

Fig. 4: Confocal microscopy images of MDA-MB-231 cells were exposed to SWCNTs-DOX, SWCNTs-DOX-HA or free DOX (DOX=40 µg/mL) for 3 h at 37 °C.

from both SWCNTs-DOX and SWCNTs-DOX-HA were stable and the release ratios were only about 11 % and 8 % within 24 h. While in pH 5.5 PBS (Fig. 2B), the release rate of DOX from SWCNTs-DOX-HA significantly increased to 34.5 % within 24 h, and the release rate of DOX from SWCNTs-DOX was 40.7% within 24 h.

2.3. *In vitro cellular uptake*

To quantitatively evaluate the HA targeting capability, MDA-MB-231 cells were incubated with SWCNTs-DOX, SWCNTs-DOX-HA or free DOX for 3 h at 37 °C. Flow cytometry was utilized to quantify the cellular uptake of SWCNTs-DOX-HA complexes via the unique red fluorescence signal of DOX. As illustrated in Fig. 3, free DOX (positive control) showed the highest cellular uptake, which indicated that hydrophilic DOX can readily diffuse into cells. Higher cellular uptake efficiency of DOX was observed in the SWCNTs-DOX-HA group compared with SWCNTs-DOX group (p<0.01). More detailedly, the SWCNTs-DOX-HA achieved a 2.1 fold increase in cellular DOX fluorescent intensity than SWCNTs-DOX. The accumulation and distribution of SWCNTs-DOX, SWCNTs-DOX-HA and free DOX in MDA-MB-231 cells were also investigated via confocal microscopic imaging of the red fluorescence of DOX and the blue fluorescence of Hoechst 33258 for cell nuclei. Figure 4 shows the intracellular fluorescence intensity of DOX, free DOX (positive control) manifested the highest fluorescence intensity, which further indicated that DOX can directly pass into the cells by a passive diffusion mechanism. The DOX fluorescence signals for SWCNTs-DOX-HA treated cells were detected at the nuclei and the perinuclear region. And the cells treated with SWCNTs-DOX-HA displayed higher fluorescence intensity than cells treated by SWCNTs-DOX. The results were consistent with the quantitative study of cellular uptake obtained by flow cytometry.

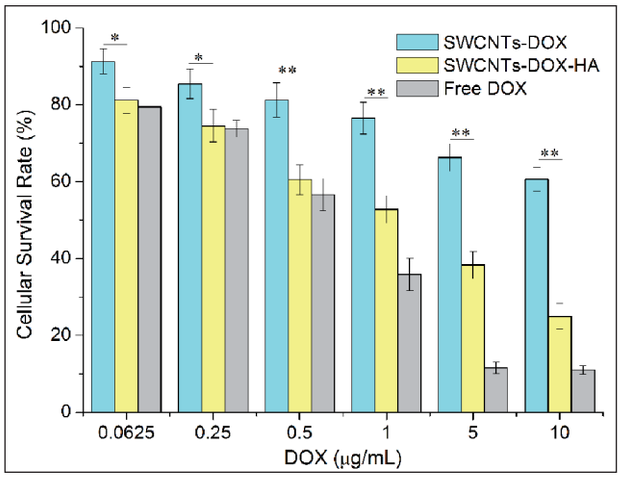

Fig. 5: Viabilities of MDA-MB-231 cells after treatment by various DOX formulations. Each bar denotes mean ±SD, (n=3). *p<0.05 and **p<0.01.

2.4. *In vitro cytotoxicity assay*

The *in vitro* cytotoxicity of SWCNTs-DOX-HA was determined by SRB assay. The cellular survival rate results are demonstrated in Fig. 5. Free DOX as positive control showed the highest cytotoxicity as DOX transferred into cells by passive diffusion and inhibited the growth of cells rapidly. Both SWCNTs-DOX-HA and SWCNTs-DOX inhibited the growth of cells in a dose-dependent manner. However, SWCNTs-DOX-HA displayed higher cytotoxicity than SWCNTs-DOX, especially when the concentration of DOX was higher than 1.0 μg/mL.

2.5. *In vitro apoptosis measurement*

The degree of *in vitro* apoptosis was quantitatively measured by flow cytometry with Annexin V-FITC/7-AAD staining. The results are shown in Fig. 6, the apoptosis rates of the control, SWCNTs-DOX, SWCNTs-DOX-HA and free DOX groups were 2.33±0.56 %, 9.25±1.62 %, 37.72±1.03 % and 73.45±1.54 %, respectively.

2.6. *Inhibition of migration of MDA-MB-231 cells*

The effect of DOX on MDA-MB-231 cells metastasis *in vitro* was investigated through the migration assay. Figure 7 depicts the wound-healing response of MDA-MB-231 cells at different time points after applying different DOX formulations. As observed in the images from the wound healing assays (Fig. 7A), SWCNTs-DOX and SWCNTs-DOX-HA failed to close the wound after 24 h and 48 h, and free DOX (positive control) displayed strongest metastatic inhibition effect. At 48 h, the migration indexes (Fig. 7B) of control, SWCNTs-DOX, SWCNTs-DOX-HA and free DOX were 73.8±0.88 %, 47.4±0.78 %, 28.6±0.32 % and 14.8±0.56 %, respectively. The migratory abilities of the MDA-MB-231 cells significantly decreased following treatment

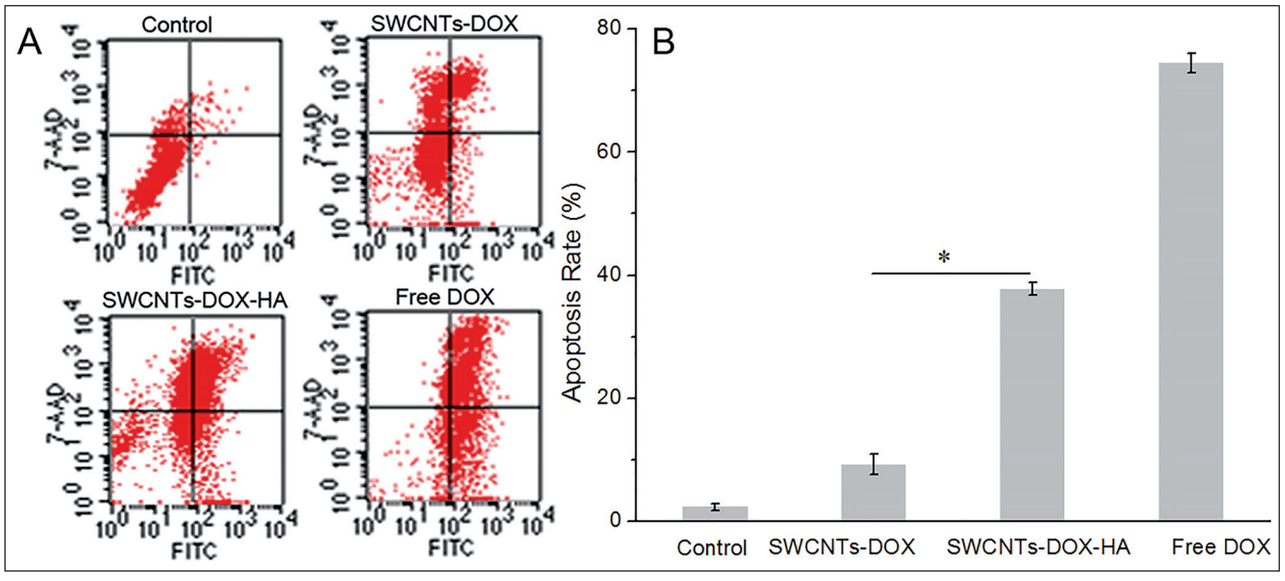

Fig. 6: The results of *in vitro* apoptosis measurement. (A) *In vitro* apoptotic analysis of each group; (B) Comparison of *in vitro* apoptosis rate of each group. Each bar denotes mean ±SD, (n=3). *p<0.01.

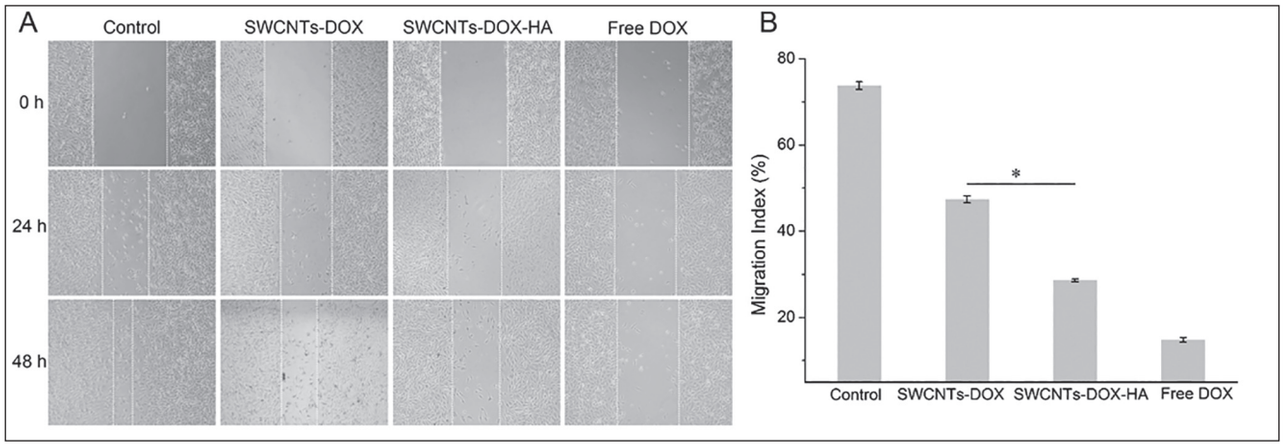

Fig. 7: The influence of varying DOX formulations on wound-healing of MDA-MB-231 cells. (A) Images of the wound healing assays; (B) Statistical analysis of migration index at 48 h. Each bar denotes mean ±SD, (n=3). *p<0.05.

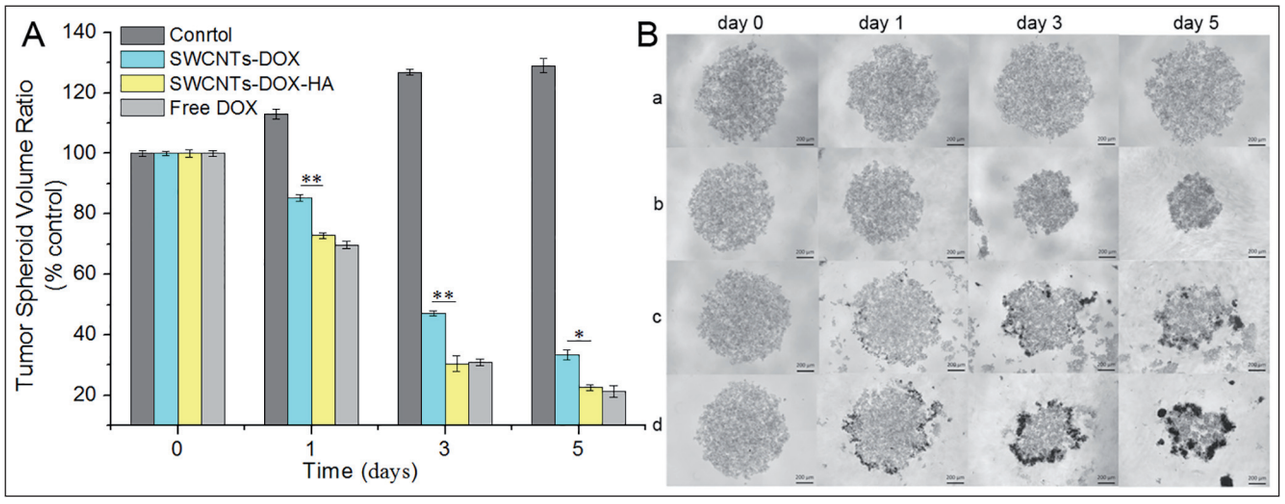

Fig. 8: Inhibitory of varying DOX formulations on MDA-MB-231 cell spheroids. (A) Inhibitory and effect on the growth of MDA-MB-231 cell spheroids. Each bar denotes mean ±SD, (n=3). *p<0.05 and **p<0.01. (B) The MDA-MB-231 cell spheroids images treated with varying DOX formulations under inverted microscope. (a) Control; (b) Free DOX; (c) SWCNTs-DOX and (d) SWCNTs-DOX-HA.

with SWCNTs-DOX and SWCNTs-DOX-HA compared with control, and SWCNTs-DOX-HA displayed stronger inhibitory effect on the migration than SWCNTs-DOX.

2.7. Anti-tumor efficiency on cancer cell spheroids

MDA-MB-231 cell spheroids were applied to assess the *in vitro* anti-tumor efficiency of SWCNTs-DOX-HA complexes. The morphology of spheroids and volume changes of control, SWCNTs-DOX, SWCNTs-DOX-HA and free DOX groups are shown in Fig. 8. After cultured for 5 days, the volume of spheroids in control group increased about 1.2 fold. While applying free DOX, SWCNTs-DOX and SWCNTs-DOX-HA, the volume of spheroids reduced sharply. Free DOX showed the highest anti-tumor efficiency. And SWCNTs-DOX-HA displayed notable inhibition effect on the growth of cell spheroids than SWCNTs-DOX. The spheroids became irregular and smaller, finally broke into pieces at day 5, implying that SWCNTs-DOX-HA could penetrate deep to the center of cell spheroids and induce cell apoptosis.

3. Discussion

The morphologies of the samples have changed greatly after every functionalization steps (Fig. 1), indicating that a targeting SWCNTs-DOX-HA drug delivery system was successfully constructed. The data of zeta potential (Table) determinations could also indicate the preparation process of SWCNTs-DOX-HA complexes. DOX, a cationic anthracycline antibiotic, combine with SWCNTs by π–π stacking interactions, van der Waals interactions, and hydrophobic interactions (Ji et al. 2012; Mehra et al. 2014; Yu et al. 2016; Zhou et al. 2012). Nano-NH_2-SWCNT is an electropositive complex. After loading DOX onto the Nano-NH_2-SWCNTs, the zeta potential of the complex increased obviously, indicating the successful combination of electropositive DOX onto the Nano-NH_2-SWCNTs. Due to multiple carboxyl groups, HA is an anionic polysaccharide polymer (Sun et al. 2012). After coated with HA, the potential decreased sharply. The reverse of surface potentials demonstrated that the HA was successfully adsorbed onto the sidewalls of SWCNTs through electrostatic adsorption. The changes in zeta potential also indicated that a targeting SWCNTs-DOX-HA drug delivery system was successfully synthesized.

After coated with HA, the sizes of complexes decreased obviously. It was probably that the SWCNTs tend to cluster into large bundles in water, so the sizes of Nano-NH_2-SWCNTs and SWCNTs-DOX were much larger than those observed by TEM. HA coating supplied a hydrophilic shield, which was helpful to improve the dispersion of SWCNTs in water. On the other hand, the zeta potential of SWCNTs-DOX-HA was below -55 mV. According to the zeta potential theory, the larger the absolute value of the zeta potential is, the more stable the system will be (Mo et al. 2015). The SWCNTs-DOX-HA's absolute value of the zeta potential was larger than Nano-NH_2-SWCNTs's and SWCNTs-

DOX's, suggesting that the SWCNTs-DOX-HA complexes would be stable in water and would not readily agglomerate. The PDI value of SWCNTs-DOX-HA further provided the evidence that HA modification could improve the dispersion of SWCNTs. The DOX loading percentage was higher than 80 %, indicating that the SWCNTs had a high loading capacity and could deliver a large amount of drug. The result was higher than previous report (Mo et al. 2015).

The results of DOX release from the SWCNTs drug delivery systems demonstrated that the release rate of DOX from SWCNTs-DOX was higher than that from SWCNTs-DOX-HA. The reason might be HA on the surface of SWCNTs-DOX acted as a shell, which reduced the release rate of DOX. The HA coating could prolong the blood circulation for the SWCNTs-DOX drug delivery system. These results indicated that SWCNTs-DOX-HA had a characteristic of pH-trigger drug release, which could increase the cytotoxic activity of the DOX at reduced pH tumor microenvironments and intracellular organelles of lysosomes and endosomes. Under normal physiological conditions in blood circulation and normal tissues, the DOX was retained on the SWCNTs and lowered the toxic and side effect to normal cells (Yao et al. 2014). The different release profiles at two PH microenvironments indicated that the pH-triggered DOX release of the SWCNTs-DOX-HA complexes is ideal choice for treating tumor with slightly acidic pH microenvironment.

During the application of carbon nanotubes (CNTs) as drug carrier, its toxicity is the key issues of their application in the therapeutic areas. In a previous study, cytotoxicity of CNTs was determined by various factors including purity, functionalization moieties, dimension, and concentration. Many reports confirmed that CNTs in lower dosages can be used as a promising drug delivery carrier for targeted therapy of cancer (Calaf et al. 2018). CD44 was overexpressed on the surface of MDA-MB-231cells. HA has been identified as an effective targeting ligand of tumors which possessed CD44 overexpressing cells (Lin Hou and Zhang 2017; Ouasti et al. 2012). The higher cytotoxicity effect of SWCNTs-DOX-HA (Fig. 5) may be due to the positive targeting resulted from the strong affinity of HA on the surface of SWCNTs to its CD44 receptor. These results revealed that the HA-mediated targeted delivery could improve the delivery efficiency of DOX and enhance therapeutic efficacy of DOX against MDA-MB-231 cancer cells, which were in good accordance with that of flow cytometry assay and confocal microscopy observation.

Free DOX could quickly pass into the cells by a passive diffusion mechanism and accumulated in the cell nucleus in great quantity, then triggered cell apoptosis by intercalating in the DNA base pairs and blocking the replication activities (Chaudhuri et al. 2010; Tacar et al. 2013; Thorn et al. 2011). The limited apoptotic effect of SWCNTs-DOX was attributed to lower cellular uptake caused by the lack of interaction between SWCNTs-DOX and the cell membrane. However, treatment with SWCNTs-DOX-HA resulted in greatly heightened apoptosis as the receptor/ligand interaction between the HA and the CD44 on the surface of cell membranes, which resulted in improved cellular uptake of the complexes. These results were in accordance with *in vitro* cytotoxicity results. Our data implied that the HA modification was effective to increase the apoptosis of DOX-loaded SWCNTs against CD44 receptor-overexpressing MDA-MB-231 cells.

A majority of cancer-associated deaths was caused by cancer metastasis (Singh et al. 2017). MDA-MB-231 is a human highly metastatic breast cancer cell line. Inhibition of migration of MDA-MB-231 cells is significant to breast cancer treatment. DOX has been reported to play an important role on the metastasis of tumor cells (Pistone et al. 2016). The migration assay results indicated that the untreated control MDA-MB-231 cells moved into scratched gaps and narrow the gaps due to their high migratory potential, while DOX could effectively inhibit the self-renew of cells and the healing of wound. It could be concluded that SWCNTs-DOX-HA had stronger inhibitory effect on the migration than SWCNTs-DOX, which proved effective anti-metastatic potential of the SWCNTs-DOX-HA formulation.

Cancer cell spheroids, 3D architectures of cancer cells, are found in many cancer patients with sizes of 250–750 µm. Unlike classical cell culture- based models, cancer cell spheroid can reflect the therapeutically relevant pathophysiological gradients. So cancer cell spheroid model was widely used as an appropriate tool to estimate the anti-tumor efficiency in drug development processes (Friedrich et al. 2009; Kou et al. 2017; Perche and Torchilin 2012). As tumor drug resistance mechanisms, the efficacy of cancer chemotherapy is poor towards many solid tumors from the beginning or following initial success, the tumor tissue is an obstacle to overcome (Mellor and Callaghan 2011; Meng et al. 2012). In this study, the targeting drug delivery system SWCNTs-DOX-HA can specifically bind to CD44 receptor and enhance uptake by MDA-MB-231 cells via CD44 receptor-mediated endocytosis, deliver the DOX penetrate deep to the center of cell spheroids and induce cell apoptosis. This model can simulate the situation observed in patients or in preclinical tumor-bearing animals. These results provide an idea for the further study of SWCNTs-DOX-HA in tumor-bearing animals.

In this study, a simply and non-covalently functionalized SWCNTs with HA for targeted delivery of DOX into CD44 overexpressing cancer cells was developed. Via the electrostatic interaction between the amino groups of SWCNTs and carboxyl groups of HA, targeting ligand HA was adsorbed onto the surface of SWCNTs successfully. The formed SWCNTs-DOX-HA complexes possessed high load capacity for DOX through π–π stacking interactions between DOX and SWCNTs, and displayed a pH-triggered DOX release characteristic with a faster DOX release rate at lower pH condition. When compared to unmodified SWCNTs-DOX, the SWCNTs-DOX-HA exhibited a significant improvement in intracellular delivery of DOX in the CD44 overexpressing MDA-MB-231 cells. More importantly, the multifunctional SWCNTs-DOX-HA complexes exerted stronger effects in inducing growth inhibition and apoptosis than SWCNTs-DOX. Also, the migration and the formation of cancer cell spheroids for MDA-MB-231 cells were significantly blocked by SWCNTs-DOX-HA. These properties endue SWCNTs-DOX-HA with precise and efficient DOX delivery for tumor cells, which hold a great promise to improve therapeutic efficacy and decrease toxicity for chemotherapy.

4. Experimental

4.1. Materials

Amino single-walled carbon nanotubes (NH_2-SWCNTs, purity > 95%, length 1-3 µm, diameter 1-2 nm) were purchased from XFNANO Co., Ltd (Nanjing, China). Doxorubicin hydrochloride (DOX) was supplied by Meilun Biotechnology Co., Ltd (Dalian, China). Hyaluronan (HA, 0.1-0.2´10^6 Da) was obtained by Dongyuan Biotech Co., Ltd (Zhenjiang, China). Agarose, Hoechst 33258, sulforhodamine B (SRB) were purchased from Sigma-Aldrich (St. Louis, USA). Ultrapure deionized (D.I.) water was generated using a plus system (Milli-Q, Millipore, Germany).

MDA-MB-231 (human breast cancer) cell line was purchased from the Cell Bank of the Chinese Academy of Sciences (Shanghai, China). The MDA-MB-231 cells were cultured in Leibovitz's L15-medium (L15, Macgene) supplemented 10% foetal bovine serum (FBS, Wisent) and 100 U/mL penicillin and 100 µg/mL streptomycin (Macgene). The cell line was cultured in a humidified incubator at 37 °C and an atmosphere of 5% CO_2.

4.2. Preparation of SWCNTs drug delivery systems

4.2.1. Loading of DOX onto NH_2-SWCNTs

Firstly, 200 mg NH_2-SWCNTs was dispersed in 200 mL anhydrous ethanol by sonication for 1 h. Then the obtained solution was processed with ultra high pressure homogenizer (Nano, DeBEE, USA) to obtain nanosize NH_2-SWCNTs. After that the nano-NH_2-SWCNTs were collected by centrifugation at 5000 r/min for 10 min, washed with PBS for three times to remove the residual ethanol. Nano-NH_2-SWCNTs (10 mg) were dispersed in 5 mL PBS and 1.3 mL of DOX (5 mg/mL in PBS) was added to the nano-NH_2-SWCNTs PBS solution. The mixture was sonicated for 30 min and stirred at room temperature for 24 h. At last, the products were collected by centrifugation, washed with D.I. water several times until the supernatant became colorless, and collected all the supernatant. The obtained SWCNTs-DOX were dispersed in 10 mL D.I. water and stored at 4 °C.

4.2.2. Preparation of SWCNTs-DOX-HA

HA solution (2 mL, 1 mg/mL) was added to 2 mL SWCNTs-DOX solution, sonicated for 30 min and stirred at room temperature for 24 h. The products (SWCNTs-

DOX-HA) were collected by centrifugation, washed with D.I. water three times. The resultant SWCNTs-DOX-HA complexes were dispersed in 2 mL D.I. water and stored at 4 °C.

4.3. Characterization of SWCNTs drug delivery systems

Particle sizes, polydispersity indexes (PDI) and zeta potentials of the different SWCNTs were measured by dynamic light scattering (DLS) analysis using Nicomp 380 ZLS particle sizing system (PSS, CA, USA). The morphologies of all SWCNTs were taken by H7700 transmission electron microscopy (Hitachi, Tokyo, Japan).

4.4. Drug encapsulation efficiency measurement

The encapsulation efficiency (EE) of DOX in SWCNTs was measured by spectrophotometry. The supernatant that contained unbound free DOX in step "loading of DOX onto NH_2-SWCNTs" was collected. The amount of free DOX that unloaded on SWCNTs was determined at 485 nm using UV-2550 spectrophotometer (SHIMADZU, Japan). The encapsulation efficiency (EE) of DOX was calculated with the following equation: EE=(weight of total DOX-weight of free DOX)/weight of total DOX×100%

4.5. In vitro release of DOX

In vitro release of DOX from SWCNTs-DOX and SWCNTs-DOX-HA was determined by a dialysis method. 1.0 mL of free DOX, SWCNTs-DOX or SWCNTs-DOX-HA solution and 2 mL of L15 medium with 10 % FBS were transferred into dialysis bag (MWCO=12,000-14,000Da). Then, the dialysis bag (end-sealed) was placed into 30 mL of pH 7.4 or 5.5 PBS with 0.2 % Tween 80 (Wt/Vol) at 37 °C under 100 rpm stirring. At certain time points, 1 mL of release medium was taken and added the same aliquot of fresh release medium. The concentration of DOX in each sample was measured by ACQUITY UPLC (Waters, USA) using fluorescent detector (excitation wavelength at 495 nm and emission wavelength at 545 nm). The mobile phase was consisted of 60% methanol, 35% water and 5% acetic acid.

4.6. In vitro cellular uptake

The targeting efficiency of different DOX loaded SWCNTs was assayed by flow cytometry. Briefly, 5×10^5 of MDA-MB-231 cells (per well) were seeded into 6-well plates. After cultured for 24 h, SWCNTs-DOX, SWCNTs-DOX-HA and free DOX (final concentration of DOX: 40 μg/mL) solutions were added to the cells, respectively. After incubation 3 h at 37 °C, the cells were washed, trypsinized, collected, and dispersed in PBS. The fluorescence intensity of DOX was determined by a flow cytometry (Becton Dickinson, NJ, USA) with 10,000 of cells were collected.

The distribution image of DOX in MDA-MB-231 cells was taken by a confocal fluorescent microscope. Briefly, $5´10^5$ of MDA-MB-231 cells (per well) were seeded into glass-base dishes and cultured for 24 h at 37 °C. SWCNTs-DOX, SWCNTs-DOX-HA and free DOX (final concentration of DOX 40 μg/mL) solutions were added to the cells, respectively. After incubation 3 h at 37 °C, the cells were washed by cold PBS three times, fixed by 4% paraformaldehyde for 20 min at 37 °C and stained cell nuclei with Hoechst 33258 (10 μg/mL) for 20 min at 37 °C. Then, images of the cells were taken by a laser confocal microscopy (Zeiss, Jeantown, Germany).

4.7. In vitro cytotoxicity of SWCNTs drug delivery systems

The *in vitro* cytotoxicities of different DOX formulations were evaluated by SRB assay. 5×10^3 of MDA-MB-231 cells (per well) were seeded into 96-well plate and cultured for 24 h. The cells were treated with different concentrations of SWCNTs-DOX, SWCNTs-DOX-HA and free DOX for 48 h. The cells were fixed by 10% cold trichloroacetic acid (Wt/Vol), washed with D.I. water and dried at room temperature. Then, the cells were stained with 0.4 % SRB (Wt/Vol) for 30 min and washed with 1 % acetic acid (Wt/Vol) several times until the solution became colorless. Finally, Tris base (10 mM) was added to each well and the 96-well plate was shaken for 30 min at room temperature. The optical density was taken by a microplate reader of multi-wavelength measurement system (Tecan, Diken, Austria). All experiments were repeated three times.

4.8. In vitro apoptosis measurement

The *in vitro* apoptosis were measured by flow cytometry with Annexin V-FITC/7-AAD staining. Briefly, the MDA-MB-231 cells were treated with SWCNTs-DOX, SWCNTs-DOX-HA and free DOX at final DOX concentration of 10 μg/mL. After incubation 24 h, the cells were washed, trypsinized, collected, and dispersed in PBS. The cells were stained with Annexin V-FITC and 7-AAD according to the apoptosis assay kit (Cwbiotech, Jiangsu, China). Then, cells were analyzed by a flow cytometry (Becton Dickinson, NJ, USA).

4.9. Inhibition of migration of MDA-MB-231 cells

$2.5´10^5$ of MDA-MB-231 cells (per well) were seeded into 12-well plate and cultured for 24 h. A single scratch wound was created in the monolayer cells using a sterile pipette tip. Cells were washed with PBS three times to remove the debris. Then, the remaining cells were cultured with L15 medium containing 2 % FBS with SWCNTs-DOX, SWCNTs-DOX-HA and free DOX (final concentration of DOX: 2 μg/mL). Images of the cells were taken by inverted fluorescence microscope (Zeiss, Jeantown, Germany) at 0 h, 24 h and 48 h. The scratch area was measured by Image J software to evaluate the effect of different DOX formulations on the cell metastatic potential.

4.10. Formation of cancer cell spheroids

Cancer cell spheroids were developed via reported method. Typically, 50 μL of 1.5 % agarose solution (Wt/Vol) in serum-free media were added to 96-well plate, and then the plate was stored for 60 min to cool down to room temperature. L15 complete medium (200 μL) containing with 5,000 cells was added to each well. Then the 96-well plate was centrifuged at 1500 x g for 15 min. L15 medium (100 μL) containing 10 % FBS was replaced gently every two days. After forming the cancer cell spheroids for about 4 days, SWCNTs-DOX, SWCNTs-DOX-HA and free DOX (final concentration of DOX: 2 μg/mL) were added to the 96-well plate. Images of the cancer cell spheroids were taken by inverted fluorescence microscope (Zeiss, Jeantown, Germany) over the following 5 days.

4.11. Statistical analysis

All the experiments were repeated for three times at least. The data were presented as mean±SD. Statistical comparisons were performed by Student's t-test. Date with of P value < 0.05 or 0.01 was considered statistically significant or very significant difference.

Acknowledgements: This research was funded by Scientific Research Fund of Heilongjiang Provincial Education Department, China (Grant NO. 2016-KYYWF-0867, 2017-KYYWF-0694) and University Nursing Program for Young Scholars with Creative Talents in Heilongjiang Province, China (Grant NO. UNPYSCT-2015108).

Conflict of interest: The authors declare that there are no conflicts of interest.

References

Assanhou AG, Li WY, Zhang L, Xue LJ, Kong LY, Sun HB, Mo R, Zhang C (2015) Reversal of multidrug resistance by co-delivery of paclitaxel and lonidamine using a TPGS and hyaluronic acid dual-functionalized liposome for cancer treatment. Biomaterials 73: 284-295.

Cai DF, Gao W, He B, Dai WB, Zhang H, Wang XQ, Wang JC, Zhang X, Zhang Q (2014) Hydrophobic penetrating peptide PFVYLI-modified stealth liposomes for doxorubicin delivery in breast cancer therapy. Biomaterials 35: 2283-2294.

Calaf GM, Ponce-Cusi R, Abarca-Quinones J (2018) Effect of curcumin on the cell surface markers CD44 and CD24 in breast cancer. Oncol Rep 39: 2741-2748.

Cao XY, Tao L, Wen SH, Hou WX, Shi XY (2015) Hyaluronic acid-modified multi-walled carbon nanotubes for targeted delivery of doxorubicin into cancer cells. Carbohydr Res 405: 70-77.

Chaudhuri P, Soni S, Sengupta S (2010) Single-walled carbon nanotube-conjugated chemotherapy exhibits increased therapeutic index in melanoma. Nanotechnology 21.

Chen C, Xie XX, Zhou Q, Zhang FY, Wang QL, Liu YQ, Zou YN, Tao Q, Ji XM, Yu SQ (2012) EGF-functionalized single-walled carbon nanotubes for targeting delivery of etoposide. Nanotechnology 23: 12.

Dvash R, Khatchatouriants A, Solmesky LJ, Wibroe PP, Wei M, Moghimi SM, Peer D (2013) Structural profiling and biological performance of phospholipid-hyaluronan functionalized single-walled carbon nanotubes. J Control Release 170: 295-305.

Firme CP, 3rd, Bandaru PR (2010) Toxicity issues in the application of carbon nanotubes to biological systems. Nanomedicine 6: 245-256.

Friedrich J, Seidel C, Ebner R, Kunz-Schughart LA (2009) Spheroid-based drug screen: considerations and practical approach. Nat Protoc 4: 309-324.

Huang J, Zhang H, Yu Y, Chen Y, Wang D, Zhang G, Zhou G, Liu J, Sun Z, Sun D, Lu Y, Zhong Y (2014) Biodegradable self-assembled nanoparticles of poly (D,L-lactide-co-glycolide)/hyaluronic acid block copolymers for target delivery of docetaxel to breast cancer. Biomaterials 35: 550-566.

Ji ZF, Lin GF, Lu QH, Meng LJ, Shen XZ, Dong L, Fu CL, Zhang XK (2012) Targeted therapy of SMMC-7721 liver cancer *in vitro* and in vivo with carbon nanotubes based drug delivery system. J Colloid Interface Sci 365: 143-149.

Kou L, Yao Q, Sivaprakasam S, Luo Q, Sun Y, Fu Q, He Z, Sun J, Ganapathy V (2017) Dual targeting of l-carnitine-conjugated nanoparticles to OCTN2 and ATB(0,+) to deliver chemotherapeutic agents for colon cancer therapy. Drug Deliv 24: 1338-1349.

Li JC, He Y, Sun WJ, Luo Y, Cai HD, Pan YQ, Shen MW, Xia JD, Shi XY (2014) Hyaluronic acid-modified hydrothermally synthesized iron oxide nanoparticles for targeted tumor MR imaging. Biomaterials 35: 3666-3677.

Lin Hou YY, Junxiao Ren, Yinling Zhang, Yongchao Wang, Xiaoning Shan, Qi Liu, Zhang Z (2017) *In vitro* and *in vivo* comparative study of the phototherapy anticancer activity of hyaluronic acid-modified single-walled carbon nanotubes, graphene oxide, and fullerene. J Nanopart Res 19: 286.

Liu Z, Robinson JT, Sun XM, Dai HJ (2008) PEGylated nanographene oxide for delivery of water-insoluble cancer drugs. J Am Chem Soc 130: 10876-10877.

Mehra NK, Mishra V, Jain NK (2014) A review of ligand tethered surface engineered carbon nanotubes. Biomaterials 35: 1267-1283.

Mellor HR, Callaghan R (2011) Accumulation and distribution of doxorubicin in tumour spheroids: the influence of acidity and expression of P-glycoprotein. Cancer Chemother Pharmacol 68: 1179-1190.

Meng E, Taylor B, Ray A, Shevde LA, Rocconi RP (2012) Targeted inhibition of telomerase activity combined with chemotherapy demonstrates synergy in eliminating ovarian cancer spheroid-forming cells. Gynecol Oncol 124: 598-605.

Mo YF, Wang HW, Liu JH, Lan Y, Guo R, Zhang Y, Xue W, Zhang YM (2015) Controlled release and targeted delivery to cancer cells of doxorubicin from polysaccharide-functionalised single-walled carbon nanotubes. J Materials Chem B 3: 1846-1855.

Mousavi SZ, Amjad-Iranagh S, Nademi Y, Modarress H (2013) Carbon nanotube-encapsulated drug penetration through the cell membrane: an investigation based on steered molecular dynamics simulation. J Membr Biol 246: 697-704.

Ouasti S, Kingham PJ, Terenghi G, Tirelli N (2012) The CD44/integrins interplay and the significance of receptor binding and re-presentation in the uptake of RGD-functionalized hyaluronic acid. Biomaterials 33: 1120-1134.

Peer D, Margalit R (2004) Loading mitomycin C inside long circulating hyaluronan targeted nano-liposomes increases its antitumor activity in three mice tumor models. Int J Cancer 108: 780-789.

Perche F, Torchilin VP (2012) Cancer cell spheroids as a model to evaluate chemotherapy protocols. Cancer Biol Ther 13: 1205-1213.

Pistone A, Iannazzo D, Ansari S, Milone C, Salamo M, Galvagno S, Cirmi S, Navarra M (2016) Tunable doxorubicin release from polymer-gated multiwalled carbon nanotubes. Int J Pharm 515: 30-36.

Qhattal HS, Liu X (2011) Characterization of CD44-mediated cancer cell uptake and intracellular distribution of hyaluronan-grafted liposomes. Mol Pharm 8: 1233-1246.

Schroeder A, Heller DA, Winslow MM, Dahlman JE, Pratt GW, Langer R, Jacks T, Anderson DG (2012) Treating metastatic cancer with nanotechnology. Nature Rev Cancer 12: 39-50.

She WC, Li N, Luo K, Guo CH, Wang G, Geng YY, Gu ZW (2013) Dendronized heparin-doxorubicin conjugate based nanoparticle as pH-responsive drug delivery system for cancer therapy. Biomaterials 34: 2252-2264.

Singh BK, Verma K, Panigrahi L, Thoke AS (2017) Integrating radiologist feedback with computer aided diagnostic systems for breast cancer risk prediction in ultrasonic images: An experimental investigation in machine learning paradigm. Exp Syst Appl 90: 209-223.

Stevens JL, Huang AY, Peng J, Chiang IW, Khabashesku VN, Margrave JL (2003) Sidewall amino-functionalization of single-walled carbon nanotubes through fluorination and subsequent reactions with terminal siamines. Nano Lett 3: 331-336.

Sun HH, Benjaminsen RV, Almdal K, Andresen TL (2012) Hyaluronic acid immobilized polyacrylamide nanoparticle sensors for CD44 receptor targeting and pH measurement in cells. Bioconjugate Chem 23: 2247-2255.

Tacar O, Sriamornsak P, Dass CR (2013) Doxorubicin: an update on anticancer molecular action, toxicity and novel drug delivery systems. J Pharm Pharmacol 65: 157-170.

Thorn CF, Oshiro C, Marsh S, Hernandez-Boussard T, McLeod H, Klein TE, Altman RB (2011) Doxorubicin pathways: pharmacodynamics and adverse effects. Pharmacogenet Genomics 21: 440-446.

Wen XC, Li JP, Cai DF, Yue LL, Wang Q, Zhou L, Fan L, Sun JW, Wu YH (2018) Anticancer efficacy of targeted shikonin liposomes modified with RGD in breast cancer cells. Molecules 23: 15.

Xu WJ, Siddiqui IA, Nihal M, Pilla S, Rosenthal K, Mukhtar H, Gong SQ (2013) Aptamer-conjugated and doxorubicin-loaded unimolecular micelles for targeted therapy of prostate cancer. Biomaterials 34: 5244-5253.

Yanhua Liu JS, Wen Cao, Jianhong Yang, He Lian, Xin Li, Yinghua Sun, Yongjun Wang, Siling Wang, Zhonggui He (2011) Dual targeting folate-conjugated hyaluronic acid polymeric micelles for paclitaxel delivery. Int J Pharm 421: 160-169.

Yao HJ, Zhang YG, Sun L, Liu Y (2014) The effect of hyaluronic acid functionalized carbon nanotubes loaded with salinomycin on gastric cancer stem cells. Biomaterials 35: 9208-9223.

Yu BD, Tan L, Zheng RH, Tan H, Zheng LX (2016) Targeted delivery and controlled release of Paclitaxel for the treatment of lung cancer using single-walled carbon nanotubes. Mater Sci Eng C Mat Biol Appl 68: 579-584.

Zhang M, Wang WT, Wu F, Yuan P, Chi C, Zhou NL (2017) Magnetic and fluorescent carbon nanotubes for dual modal imaging and photothermal and chemotherapy of cancer cells in living mice. Carbon 123: 70-83.

Zhang XK, Meng LJ, Lu QH, Fei ZF, Dyson PJ (2009) Targeted delivery and controlled release of doxorubicin to cancer cells using modified single wall carbon nanotubes. Biomaterials 30: 6041-6047.

Zhou FF, Wu S, Song S, Chen WR, Resasco DE, Xing D (2012) Antitumor immunologically modified carbon nanotubes for photothermal therapy. Biomaterials 33: 3235-3242.

Zhou MJ, Zhang XJ, Yang YL, Liu Z, Tian BS, Jie JS, Zhang XH (2013) Carrier-free functionalized multidrug nanorods for synergistic cancer therapy. Biomaterials 34: 8960-8967.